ACS OMEGA

Open Access

This article is licensed under CC-BY-NC-ND 4.0

http://pubs.acs.org/journal/acsodf

Article

Nanostructured Lipid Carrier for Intracellular Delivery of a Bis(pyridine-2-carboxamidine) DNA Minor Groove Binder Active against *Leishmania*

J. Jonathan Nué-Martinez, Marta Leo-Barriga, Fernando Herranz, Zisis Koutsogiannis, Paul W. Denny, Godwin U. Ebiloma, Christophe Dardonville,* and Ana González-Paredes*

Cite This: *ACS Omega* 2025, 10, 7795−7805

Read Online

ACCESS | Metrics & More | Article Recommendations | Supporting Information

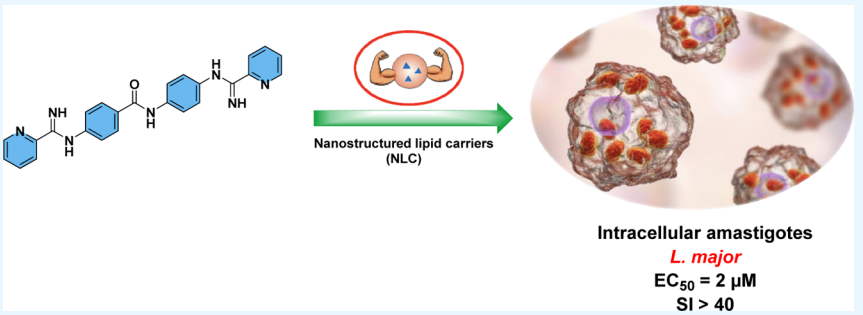

ABSTRACT: Two types of nanostructured lipid carrier (NLC) formulations of the antileishmanial DNA minor groove binding compound 4-(picolinimidamido)-*N*-(4-(picolinimidamido)phenyl)benzamide (**1**) were synthesized by the microemulsion method to evaluate their potential as a delivery system to intracellular forms of the *Leishmania* parasite. Compound **1**-loaded NLC formulations, functionalized with folic acid (FA) or not, showed good colloidal stability both during storage and after dilution in biologically relevant media. The drug release, which was not pH dependent, occurred efficiently at 37 °C. Compound **1** and its NLC formulations displayed a good selectivity index (SI > 40) and were active in the submicromolar range against promastigotes and metacyclic promastigotes of *Leishmania major* and in the low micromolar range (∼2 μM) against intramacrophage amastigotes. However, they were inactive against *Leishmania mexicana*. This proof-of-concept study showed that compound **1** could be loaded effectively in NLC and FA-coated NLC whose size and anionic nature (i.e., FA-NLC) are favorable for uptake into macrophages. NLC functionalization with FA had a beneficial effect on the antileishmanial activity of **1** compared with noncoated NLC formulations, which resulted in an increase in selectivity toward the parasite.

Downloaded via 81.158.211.175 on March 25, 2025 at 17:49:03 (UTC).
See https://pubs.acs.org/sharingguidelines for options on how to legitimately share published articles.

1. INTRODUCTION

Parasites of the genus *Leishmania* cause leishmaniasis, a neglected parasitic disease with clinical manifestations ranging from cutaneous and mucocutaneous forms to a deadly visceral form caused by *Leishmania donovani* and *Leishmania infantum*. According to the World Health Organization, approximately 700,000 to 1 million new cases and some 26,000 to 65,000 deaths occur every year.[1] The disease affects the poorest people across the world, mainly in tropical and subtropical areas. However, its distribution has evolved in recent decades due to different factors including demography and coinfections.[2,3] Current drugs to treat leishmaniasis are nonspecific and generally require prolonged therapy, resulting in high toxicities and low patient compliance. As a result, drug resistance and therapeutic failure are increasing.[3,4]

We recently reported the discovery of different families of AT-specific DNA minor groove binders active against the kinetoplastid parasites *Trypanosoma brucei*, *T. cruzi*, and *L. donovani*.[5] Among these series, 4-(picolinimidamido)-*N*-(4-(picolinimidamido)phenyl)benzamide (**1**) was chosen as the lead compound because it fulfils our hit selection criteria for the 3 parasites (i.e., EC_{50} < 5 μM and selectivity index (SI) > 50). In particular, compound **1** was the most potent and selective inhibitor of *Leishmania* growth (SI > 76) with EC_{50} values of 0.26 and 0.65 μM against promastigotes and intracellular amastigotes of *L. donovani*, respectively (Figure 1). In addition, compound **1** displayed adequate metabolic stability ($t_{1/2}$ > 2 h in human and mouse microsomes, and >1 h in human serum)[5] indicating that it is a potential candidate for in vivo studies.

Received: September 4, 2024
Revised: January 27, 2025
Accepted: February 3, 2025
Published: February 19, 2025

© 2025 The Authors. Published by American Chemical Society

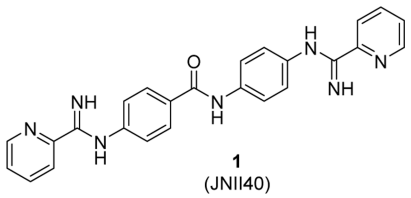

Figure 1. Structure of antileishmanial lead compound **1**.

We showed that similar to previously reported bis(2-aminoimidazoline) molecules,[6] compound **1** was able to compete with the HMGA AT-hook 1 domain for binding to the minor groove of DNA.[7] This indicates that AT-hook proteins such as LamAT-Y,[8] which are critical for the normal biology of *Leishmania* parasites, are possible targets of this molecule. The promising antileishmanial activity of **1** against visceral leishmaniasis (VL) is currently under investigation in vivo (unpublished data). However, the therapeutic potential of compound **1** against cutaneous leishmaniasis (CL) has not been studied so far. CL is a disease caused by more than 15 *Leishmania* species, which is present in nearly 90 countries worldwide.[1] CL treatment mostly relies on local applications of antileishmanial drugs (paromomycin ointment, local infiltration with antimonials), thermotherapy, and cryotherapy for patients with small and few wounds located in anatomical areas accessible to topical treatment.[9−11] Parenteral administration of pentavalent antimonials is the first-line therapy for patients with numerous or large lesions despite its high cardiac, hepatic, and renal toxicity.[9] Other (second line) treatments consist of oral miltefosine, intravenous pentamidine isethionate, amphotericin B deoxycholate or its liposomal formulation, and ketoconazole.[12] Even so, there is a need for new safe drugs and formulations for CL.

During infection, *Leishmania* promastigotes, which are inoculated in the skin by the sandfly vector, hijack mammalian host cells (i.e., macrophages and other types of mononuclear phagocytic cells) where they transform into amastigotes, replicate, and eventually break the cell to infect other tissues.[11] Hence, drugs targeting the mitochondrial DNA (kDNA) of intracellular amastigotes of *Leishmania* must cross 4 biological membranes (host cell membrane, parasitophorous vacuole membrane, parasite cell membrane, and mitochondrial membranes) to reach kDNA.

Many nanodrug delivery systems have been studied to improve the activity, bioavailability, and safety profile of antileishmanial drugs.[13] Nanostructured lipid carriers (NLCs) are versatile nanoparticles (NPs) made of a mixed matrix formed by solid and liquid lipids stabilized in water thanks to a mixture of surfactants. They form an amorphous lipid matrix that can be loaded with both lipophilic and hydrophilic drugs.[14,15] Furthermore, NLCs can be administered by different routes (e.g., oral, transdermal, ocular, intranasal, intravenous) and show very favorable toxicity profiles.[14] For instance, NLCs were used to improve the water solubility and bioavailability of antileishmanial hydroxymethilnitrofurazone (p.o. administration),[16] carvacrol (i.v.),[17] ursolic acid (i.p.[18] and p.o.[19]), or a diselenide compound (p.o.).[20] Other NLC formulations of miltefosine (p.o.),[21] amphotericin B (topical),[22] or annatto oil[23] demonstrated improved efficacy and lower toxicity against *Leishmania major* CL. In this study, we envisioned the use of NLC to improve the delivery of the DNA minor groove binding compound **1** to intracellular *Leishmania* parasites.

The selective targeting of drugs and NP formulations to parasites using specific nutrient transporters and receptors is a promising strategy to enhance the chemotherapeutic potential of drugs.[13,24−27] On the one hand, *Leishmania* species are folate auxotrophs and salvage folic acid (FA) via at least two high-affinity folate transporters (FT1 and FT2) which could be used for specific drug delivery to the parasite interior.[28,29] On the other hand, macrophages are key to the *Leishmania* life cycle; thus, a targeting approach that uses macrophage's ability to internalize specific biomolecules should improve the delivery of lead compound **1** to the parasite.[26] The surface of activated macrophages expresses the β isoform of the folate receptor (FR-β), a high-affinity receptor for FA.[30] As shown in the field of cancer chemotherapy, NP functionalized with FA is effectively internalized by activated macrophages by receptor-mediated endocytosis without promoting their uptake by other healthy cells and tissues.[31] Hence, NP decorated with FA can be exploited to target therapeutic agents to activated macrophages and, therefore, to sites of inflammation.[32,33] Although the expression of FR-β during *Leishmania* infection is dependent on various factors, including macrophage activation, we wanted to test whether NLC functionalization with FA would have a beneficial effect on the antileishmanial activity of **1** compared with noncoated NLC formulations.

Scheme 1. Synthesis of Drug-Loaded NLC (Partially Created with a Free Version of biorender.com)

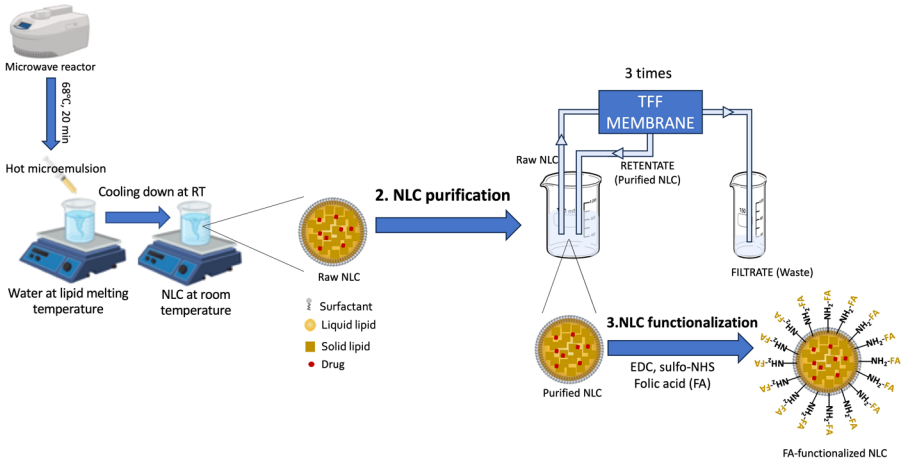

https://doi.org/10.1021/acsomega.4c08138
ACS Omega 2025, 10, 7795−7805

Table 1. Nanoparticle Characterization Data (n = 3−6 ± SD): HDD, PDI, and Zeta Potential Were Determined by DLS

formulation	HDD (nm)	PDI	Z potential (mV)	compound **1** (μM)	entrapment efficiency (%)	FA amount on NLC (w/w %)
B-NLC[a]	160 ± 15	0.289 ± 0.024	+33 ± 3			
1-NLC[b]	193 ± 18	0.315 ± 0.035	+35 ± 4	21.3 ± 8.8	16.5 ± 4.8	
FA-B-NLC[c]	131 ± 16	0.263 ± 0.039	−18 ± 2			0.85 ± 0.08
FA-**1**-NLC[d]	125 ± 18	0.257 ± 0.022	−16 ± 2	17.6 ± 8.7	14.4 ± 6.2	0.86 ± 0.01

[a]Blank NLC. [b]NLC loaded with **1**. [c]Folic acid-functionalized blank NLC. [d]Folic acid-functionalized NLC loaded with **1**.

In this study, plain and FA-functionalized NLC were synthesized by a warm microemulsion method, and a combination of techniques was used for their physicochemical characterization. Both sets were loaded with compound **1**, and two sets of blank NLC without payload (both plain and FA functionalized) were prepared as controls. All these NPs were tested against the promastigote, axenic amastigote (or metacyclic promastigote), and intracellular amastigote forms of two cutaneous *Leishmania* cell lines (*Leishmania major* and *L. mexicana*). The effect of these formulations on macrophages was also tested to determine the therapeutic index.

2. RESULTS

2.1. Synthesis and Characterization of the NLC. NLCs were synthesized by modifying the warm microemulsion method using a microwave reactor. After the synthesis, NLCs were purified by tangential flow filtration (TFF). The whole process is summarized in Scheme 1. Physicochemical characterization data for purified NLC are displayed in Table 1. The synthesized NLC, either loaded with compound **1** or blank, showed particles with hydrodynamic diameter (HDD) <200 nm but with a slightly larger size for loaded NLC (193 ± 18 nm) versus blank NLC (160 ± 15 nm) and with polydispersity index (PDI) values of approximately 0.3, which indicates a homogeneous size distribution. The zeta potential was positive (+33 and +35 mV, respectively), which confirmed the presence of octadecylamine (ODA) on the surface. The incorporation of FA on the NLC's surface was achieved by incubation of NLC with FA in the presence of EDC and sulfo-NHS at a slightly basic pH (7.5−8.0). NLC functionalization led to a reduction in particle size (≈130 nm) compared to nonfunctionalized NLC. Optimization of the incubation time needed to complete the functionalization with FA was determined by monitoring the zeta potential over 4 h, as the addition of FA caused an inversion in the zeta potential from positive to negative, reaching a plateau after 2 h of incubation (Figure S1, Supporting Information). The concentration of FA on the NLC's surface was determined spectrophotometrically (160 ± 1.8 μg/mL for blank NLC and 163 ± 0.2 μg/mL for **1**-loaded NLC). Although this concentration represented ≈16% of the initial amount of FA used in the incubation process, it proved to be enough to ensure particle functionalization, as demonstrated by zeta potential inversion. The entrapment efficiency of compound **1** was ≈15% for both plain and FA-functionalized NLC, providing a final concentration of compound **1** of 21.3 ± 8.8 μM and 17.6 ± 8.7 μM, respectively.

Morphological analysis of the developed NLC was performed by using transmission electron microscopy (TEM). Both compound **1**-loaded and blank NLC showed a spherical shape with a uniform size distribution (Figure 2), confirming the data obtained by DLS. Furthermore, no large aggregates were observed.

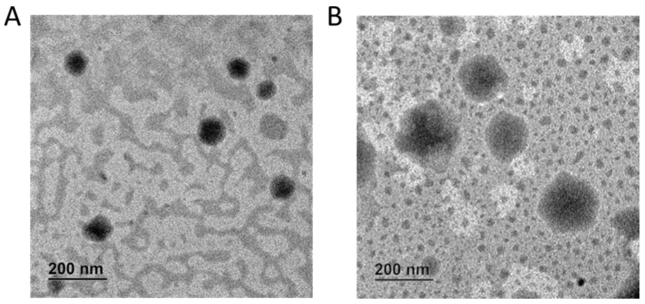

Figure 2. TEM images for blank NLC (A) and compound **1**-loaded NLC (B) formulations.

The evaluation of the physical state of the NLC lipid matrix was carried out by differential scanning calorimetry (DSC) (Figure 3). The **1**-NLC lipid matrix was totally amorphous, contrary to the solid lipids contained in the composition, which, analyzed in bulk conditions, showed a transition temperature corresponding to their melting point at 57 °C (glycerol monolaurate) and 51.5 °C (ODA), respectively.

2.1.1. In Vitro Drug Release. The release behavior at 37 °C was studied with formulation **1**-NLC at acidic (pH 5.5) and physiological pH (7.4). The stability of the NPs at these pH values was previously evaluated at room temperature (RT), with no signs of aggregation or colloidal instability during the release study (Figure S2, Supporting Information). A burst release of compound **1** was observed after 2 h of incubation at 37 °C regardless of the pH of the buffer, with 98% of the encapsulated drug released at pH 7.4 and 95% released at pH 5.5.

2.1.2. Stability Studies. Several stability studies were carried out, including colloidal stability during storage at RT and after dilution in biologically relevant buffers and media. As shown in Figure 4, both blank NLC and **1**-loaded NLC maintained their initial size during the 60 days of storage at RT, whereas the zeta potential decreased over the study period, reaching negative values at the end of the study. The same behavior in terms of size was observed for FA-functionalized NLC, maintaining the initial values during the study, whereas modifications in the zeta potential were not observed during the entire study period. After 35 days, the study with FA-functionalized NLC was interrupted because a yellow precipitate was observed at the bottom of the vial, and the percentage of remaining particles in the suspension was below 40%, although no changes in size or zeta potential were observed.

Additionally, the colloidal stability of **1**-NLC and FA-**1**-NLC in the culture media used for macrophage and parasite growth in vitro (i.e., Dulbecco's Modified Eagle's Medium (DMEM) and Schneider's insect medium (SIM), respectively) was evaluated at 37 °C for 24 h. The nonfunctionalized formulation **1**-NLC was very stable in DMEM at smaller dilutions (1:20, 1:50, and 1:100), maintaining the HDD of the

https://doi.org/10.1021/acsomega.4c08138
ACS Omega 2025, 10, 7795−7805

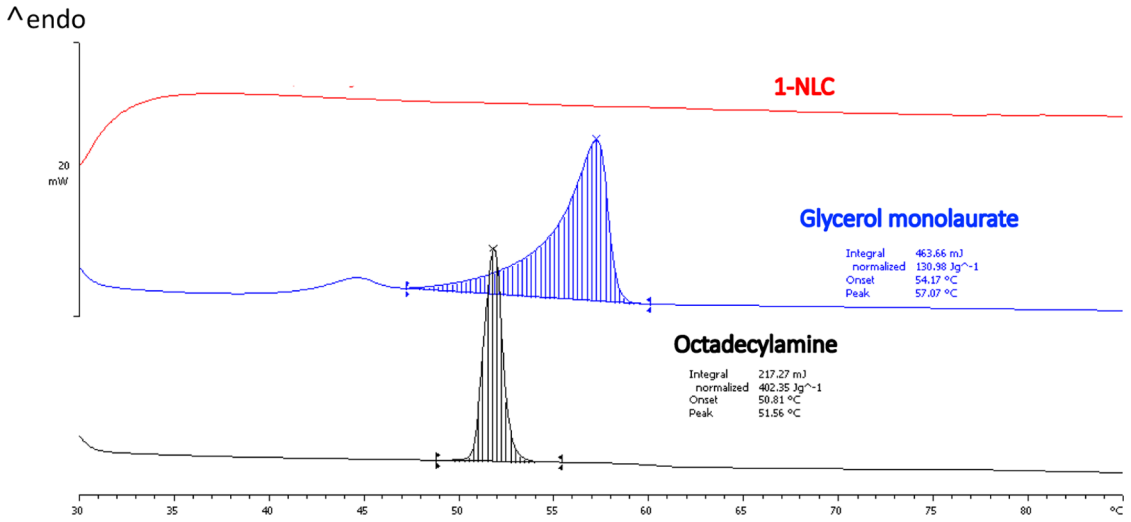

Figure 3. DSC melting curves of compound **1**-loaded NLC (red line) and bulk solid lipids: glycerol monolaurate (blue line) and ODA (black line).

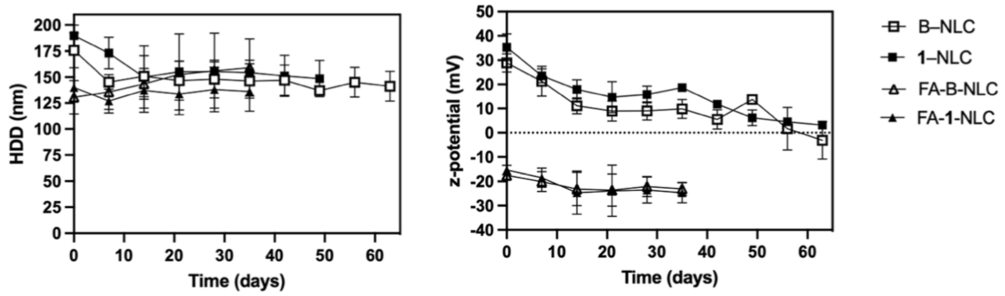

Figure 4. Evaluation of colloidal stability of the synthesized NLC formulations during storage: evolution of HDD and zeta potential over time at RT (n = 3−6 ± SD).

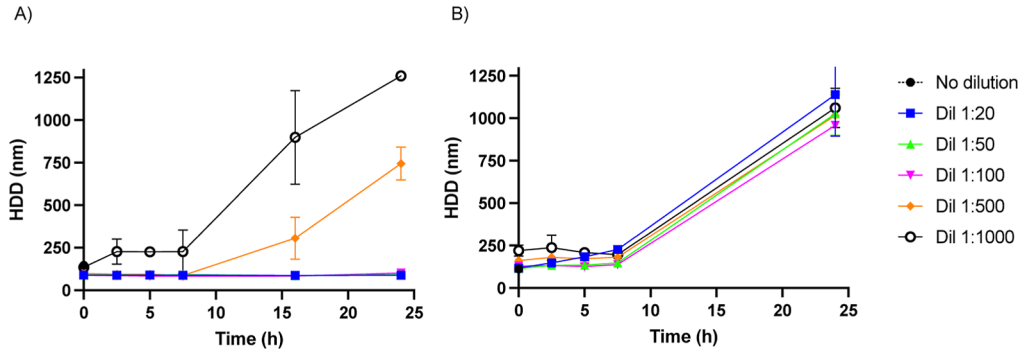

Figure 5. Colloidal stability monitoring of **1**-NLC formulation (A) and FA-functionalized 1-NLC formulation (FA-**1**-NLC) (B) in DMEM at 37 °C. Evolution of HDD over time (n = 3 ± SD).

particles unaltered during the entire study, whereas at higher dilutions (1:500 and 1:1000), progressive aggregation of **1**-NLC was observed after 15 h of incubation (Figure 5A). On the other hand, the dilution in SIM barely affected the HDD of **1**-NLC (Figure 6A). The FA-functionalized formulation FA-**1**-NLC diluted in DMEM maintained the initial HDD of the particles up to 8 h at all dilutions. After that point, progressive aggregation was observed (Figure 5B). This effect was less dramatic after dilution in SIM, where only dilution 1:100 reached HDD > 1000 nm at 24 h. In contrast, the other dilutions showed limited aggregation at the end of the study (Figure 6B).

2.2. Biology. *2.2.1. Antiprotozoal Activity.* Compound **1**, either alone or loaded in the two different types of NLC formulations, was assayed in vitro against *L. major* and *L. mexicana*, two cell lines causing CL in the Old- and New World, respectively. Blank (unloaded) NLC formulations were also tested as controls. Compound **1** inhibited the growth of promastigotes and metacyclic promastigotes of *L. major* with submicromolar EC_{50} values (0.287 and 0.438 μM), whereas it was approximately 9-times less potent against intracellular amastigotes (EC_{50} = 2.52 μM). These data were congruent with the previous results obtained against *L. donovani* ($EC_{50(promast.)}$ = 0.25 μM; $EC_{50(intra.amast.)}$ = 0.65 μM).[5] In contrast, compound **1** was completely inactive against *L. mexicana* (EC_{50} > 50 μM). Congruently, **1**−NLC, FA-**1**-NLC, B-NLC, and FA-B-NLC were tested on *L. mexicana* promastigotes and amastigotes but were found to be,

https://doi.org/10.1021/acsomega.4c08138
ACS Omega 2025, 10, 7795−7805

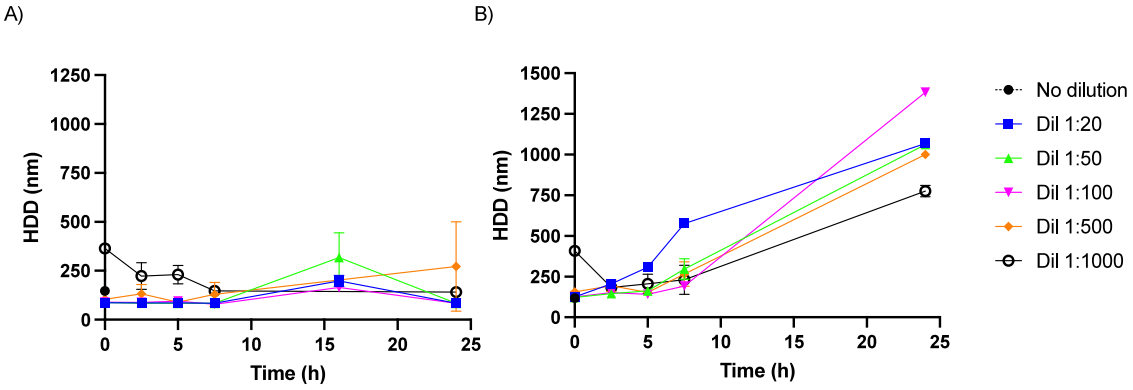

Figure 6. Colloidal stability monitoring of **1**-NLC formulation (A) and FA-functionalized 1-NLC formulation (FA-**1**-NLC) (B) in SIM at 37 °C. Evolution of HDD over time (n = 3 ± SD).

Table 2. In Vitro Antiprotozoal Activity (EC_{50}; μM)[a] and Cytotoxicity (CC_{50}; μM) against Macrophage Cells of Compound 1 and NLC Formulations

formulation	EC_{50} (μM)			CC_{50} (μM)
	L. major			macrophage[d]
	promastigote[a]	metacyclic promastigote[b]	intracellular amastigote[c]	
1	0.287 ± 0.07	0.438 ± 0.016	2.52 ± 0.22	>100
1−NLC[e]	0.253 ± 0.019	0.398 ± 0.006	2.07 ± 0.04*[f]	>100
FA-**1**-NLC[g]	0.221 ± 0.019*[f]	0.397 ± 0.012[f]	1.97 ± 0.03*[f]	>100
B-NLC[h]	5.49 ± 0.18***[i]	5.59 ± 0.25***[i]	18.9 ± 0.94***[i]	>100
FA-B-NLC[h]	4.55 ± 0.06***[i]	4.64 ± 0.05***[i]	3.58 ± 0.51**[j]	>100
AmB[k]	0.034 ± 0.003	0.056 ± 0.002	0.080 ± 0.010	>100

[a]Promastigotes of *L. major* (MHOM/IL/81/Friedlin). [b]Metacyclic promastigotes of *L. major* (MHOM/IL/81/Friedlin). [c]Intracellular amastigotes of *L. major* (MHOM/IL/81/Friedlin). [d]*Mus musculus* leukemia virus-transformed macrophage (RAW267.4) cells (ATCC TIB-71). [e]Uncoated NLC containing **1**. [f]*P*-values calculated using the unpaired Students *t*-test against compound **1**. [g]Folic acid-functionalized NLC containing **1**. [h]Blank NLC: control NLC without payload, both plain (B-NLC) and FA functionalized (FA-B-NLC). [i]P-values calculated using the unpaired Students *t*-test against compound **1**, **1**-NLC, and FA-**1**-NLC. [j]P-values calculated using the unpaired Students *t*-test against FA-**1**-NLC. [k]Amphotericin B. *P < 0.05; **P < 0.01; ***P < 0.001.

respectively, inactive (EC_{50} > 50 μM) (result not shown). This contrasting antileishmanial activity could be explained by differences between the biology of *L. mexicana* and *L. major*.[34,35]

The **1**−NLC and FA-**1**−NLC formulations produced a minimal, although significant, increase in activity against intracellular amastigotes of *L. major* (EC_{50} = 2.07 and 1.97 μM, respectively) compared to free compound **1** (EC_{50} = 2.52, P = 0.028 and 0.012, respectively, n = 4). In contrast, no significant increase in activity against extracellular promastigotes and metacyclic promastigotes was observed with these formulations (P > 0.05), except for FA-**1**−NLC (EC_{50} = 0.221 μM), which was marginally more effective against promastigotes than **1** (EC_{50} = 0.287 μM; P = 0.014).

Surprisingly, blank NLC (B-NLC), which contains no active compound **1**, displayed intrinsic activity in the low micromolar range against *L. major*, with similar EC_{50} values against promastigotes and metacyclic promastigotes (≈5.5 μM) and a 3-times higher EC_{50} value (18.9 μM) against intracellular amastigotes. In all cases, FA-B-NLCs were marginally more active (EC_{50} = 4.55 and 4.64 μM) than B-NLC (5.49 and 5.59 μM, P < 0.05) against promastigotes and metacyclic promastigotes, respectively. Likewise, FA-B-NLC was slightly more potent against intracellular amastigotes (EC_{50} = 3.58 μM) than against metacyclic promastigotes (EC_{50} = 4.64 μM, P = 0.028). The most dramatic effect of FA functionalization was observed with intracellular amastigotes, which were 5.3-fold more sensitive to blank FA-B-NLC (EC_{50} = 3.58 μM) than blank B-NLC (18.9 μM, P = 0.004, n = 4). Altogether, these results indicate that the FA coating had a positive effect on NLC uptake by macrophages (Table 2). Importantly, compound **1** and the different NLC formulations were nontoxic to macrophages up to 100 μM, indicating low toxicity with a SI > 40.

3. DISCUSSION

We have shown earlier that the DNA minor groove binding compound **1** is very effective against *L. donovani*, the parasite causing VL in the New World.[5] Here, we have shown that **1** is also active in vitro against promastigotes and amastigotes of *L. major*, a cell line causing the cutaneous form of the disease. CL treatment is challenging due to the variations in host treatment responses, which are largely due to factors that are parasite species specific. Most of the antileishmanial drugs that have been in use for decades have become ineffective with species-level insensitivity. This notwithstanding, *L. major* appears largely susceptible to most drugs currently used for treating CL. Although differences in susceptibility of Old-World (*L. donovani*,[5] *L. major*: submicromolar EC_{50}) and New-World (*L. mexicana*: inactive) *Leishmania* species toward compound **1** were observed, this was not unexpected because the importance of speciation in the treatment of leishmaniasis is well documented.[36,37] For instance, *L. mexicana* was shown to be more susceptible to azoles[38] than *L. major*, whereas it was

https://doi.org/10.1021/acsomega.4c08138
ACS Omega 2025, 10, 7795−7805

less sensitive to Amphotericin B deoxycholate[39] or stibogluconate.[37] Therefore, it could be hypothesized that a genetic variation in these parasites was responsible for the observed difference in sensitivity.

Based on several literature reports on the application of lipid-based NP to deliver leishmanicidal drugs,[40−42] we tested whether plain and FA-functionalized NLC formulations could improve the delivery (and in vitro activity) of compound **1** to intracellular *Leishmania* parasites. The in vivo fate of lipid-based NPs depends on various factors including the particle size, lipid composition, and surface decoration.[15] The particle size is a determinant in the biodistribution because NP smaller than 100 nm can escape capture by circulating macrophages. As a consequence, they can circulate in the blood for a longer time.[43−45] As far as leishmaniasis is concerned, a particle size >100 nm is required to favor the uptake (via endocytosis) by infected macrophages. The release of encapsulated bioactive compounds from the NLC is believed to occur through simultaneous diffusion from the NLC and degradation of the lipid particles in the late endosome.

In general, the NLC formulations of **1** (**1**-NLC) ($EC_{50(promast.)} \approx 0.25$ μM, $EC_{50(metacyclic\ promast.)} \approx 0.4$ μM, and $EC_{50(intra.amast.)} = 2.0$ μM, respectively) displayed in vitro potency in the same range as the free compound **1** showing that encapsulation had a modest beneficial effect on its antileishmanial activity in vitro. However, this small difference may be amplified in vivo, as was observed with other nanocarrier formulations of antileishmanial drugs. For instance, NLC formulations of cedrol resulted in a moderate 2-fold increase in SI for *L. donovani* strains versus free cedrol. In contrast, in vivo studies by oral administration in a mouse model of leishmaniasis revealed that the bioactivity of cedrol-loaded NLC increased 2.3- to 3.8-fold in the wild type and 3- to 4.9-fold in drug-resistant strains as opposed to free cedrol.[42] AmBisome, the liposomal formulation of amphotericin B, is another example of the amplification of the antileishmanial activity and safety in vivo by a nanocarrier formulation. AmBisome, which was three to six times less active in vitro than free amphotericin B against both *L. major* promastigotes and intramacrophage amastigotes, produced a dose−response effect between 6.25 and 50 mg/kg when administered once a day (i.v.) on six alternate days. In contrast, the free drug was ineffective at nontoxic doses.[46] More recently, NLC formulation of amphotericin B, which displayed similar IC_{50} values against *Leishmania braziliensis* as free AmB, showed a higher SI and lower toxicity to host cells and effectively reduced both lesion size and parasite load in a murine model of CL.[47] Thus, NLC formulations appear as a promising (and possibly cheaper) alternative to existing liposomal formulations of antileishmanial drugs. Altogether, the fact that the in vitro activity of **1**-NLC and FA-**1**-NLC was maintained, and slightly improved against infected cells in vitro, shows that the in vivo analysis of the NLC formulations of compound **1** is warranted.

A closer analysis of the in vitro results showed an interesting difference between plain and FA-functionalized NLC. On the one hand, the slightly lower EC_{50} values (1.3-fold, $P < 0.05$) against extracellular parasites of FA-**1**-NLC ($EC_{50(promast.)} = 0.221$ μM) versus **1** ($EC_{50(promast.)} = 0.287$ μM), compared to **1**-NLC versus **1** (∼1.1-fold, $P > 0.05$) support the hypothesis that NP uptake into parasite cells depends on a different mechanism that might involve, in part, the folate transporters of *Leishmania*.[48,49] On the other hand, the higher potency improvement of the FA-**1**-NLC encapsulated drug toward intracellular amastigotes ($EC_{50(intra.amast.)} = 2.07$ μM) is possibly linked to increased uptake by macrophages. On one side, a specific interaction with the folate receptor of macrophages would be expected to provide a high potency enhancement toward FR-positive cells, as observed in the field of FR-targeted anticancer chemotherapy,[50−52] unless a reduced expression of the FR is present on resident macrophages. However, the activity enhancement could also occur via an unspecific mechanism related to the size and surface charge of these NPs. It is well established that solid lipid nanoparticles (SLNs) with a size <200 nm are efficiently phagocytosed by macrophages and can be uptaken by *Leishmania*-infected macrophages.[53] Pires et al. observed that the lipidic nature, negative charge, and diameter of particles (∼100 nm) are the main characteristics that favored internalization of their SLN into macrophages.[54] Furthermore, phagocytic cells take up anionic NP to a higher extent than nonphagocytic cells which have a preference for cationic NP.[55] Hence, the size (∼125 nm) and negative nature (Z ∼ −16 mV) of the FA-functionalized compound **1**-loaded formulation, FA-**1**-NLC, probably favor its internalization into macrophages versus nonfunctionalized NLCs which are cationic (∼190 nm; Z ∼ +35 mV). This trend is illustrated by the 5.3-fold lower EC_{50} value of unloaded FA-B-NLC (3.58 μM) versus B-NLC (18.9 μM) against intracellular amastigotes (Table 2). The fact that FA-B-NLC was slightly more potent against intracellular amastigotes (3.58 μM) than metacyclic promastigotes (4.64 μM; $P = 0.028$) is also consistent with these observations.

Notably, the intrinsic micromolar in vitro antileishmanial activity of the blank NPs against extracellular and intracellular *L. major* parasites (Table 2) could be due to the lipid matrix composition, the presence of 12% surfactants in the formulation, and the combination of both. Oliveira et al.[56] linked the antileishmanial activity of essential oils from *Scheelea phalerata* to their lipid composition, whereas Ferreira et al. attributed the antileishmanial effect of unloaded cetyl palmitate and myristyl myristate-based SLN to the high surfactant content (i.e., ca. 11% w/w poloxamer) of their formulations.[23] Moreover, Serrano et al.[57] have shown a strong leishmanicidal activity of lauric acid and a moderate activity of polysorbate 20 on three different extracellular forms of the parasite *Leishmania amazonensis*, *L. braziliensis*, and *L. donovani*. Remarkably, the leishmanicidal activity displayed by the compounds present in the NLC composition is a potential advantage that might boost the activity of compound **1** once it has been taken up by the cells.

DSC experiments showed that the prepared NLCs have an amorphous matrix, suggesting that a high incorporation of the compound into the NLC core should occur, as previously demonstrated when comparing SLN with NLC in terms of drug loading and entrapment efficiency.[58,59] However, the entrapment efficiency of compound **1** was limited (≈15%), even though the incorporated amount (21.3 and 17.6 μM for plain and FA-derivatized NLC, respectively) was >40 times and >7 times higher than compound's **1** EC_{50} value against metacyclic promastigotes and intracellular amastigotes of *L. major*, respectively. Hence, the measured colloidal stability behavior of the NLC and the release profile of **1** should ensure the appropriate availability of compound **1** once it is taken up by the cells. The incorporation of compound **1** in NLC did not substantially change the physicochemical properties of the NLC, with a HDD (193 ± 18 nm) similar to that of the blank formulation (160 ± 15 nm). However, FA functionalization of

https://doi.org/10.1021/acsomega.4c08138
ACS Omega 2025, 10, 7795−7805

Scheme 2. Synthesis of Compound 1

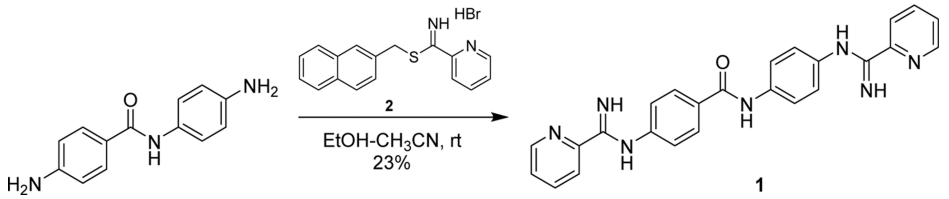

the NLC surface caused a reduction in particle size (125 ± 18 and 131 ± 16 nm, respectively).

4. CONCLUSIONS

This proof-of-concept study showed that compound **1** can be loaded effectively in NLC and FA-coated NLC in which the size and anionic nature (i.e., FA-NLC) are favorable for uptake into macrophages. These formulations retained an excellent antileishmanial in vitro activity ($EC_{50} \leq 2$ μM) against promastigotes, metacyclic promastigotes, and intracellular amastigotes of *L. major*, indicating an effective release of the active compound. This was accompanied by a small (statistically significant) improvement in the therapeutic index of **1** against *L. major*-infected macrophages. Since it is expected that activity enhancement and/or safety profile may be amplified in vivo, as was observed with other nanocarrier formulations of antileishmanial drugs (e.g., amphotericin B), further studies of this kind of formulations are warranted to optimize the delivery of this class of compounds in vivo. Of note, the lack of activity of **1** toward *L. mexicana* seems to indicate that Old World *Leishmania* cell lines (e.g., *L. donovani*,[5] *L. major*) are particularly susceptible to this compound.

5. MATERIALS AND METHODS

5.1. General. Lauroglycol 90 (propylene glycol monolaurate) was a gift from Gattefossé Spain (Madrid, Spain), whereas Tween 20 (polyoxyethylene (20) sorbitan monolaurate) and Myrj 40 (polyoxyethylene (40) Stearate) were kindly donated by Croda Iberica (Barcelona, Spain). SUNSOFT 750 (glycerol monolaurate) was a gift from Kagaku (Japan). ODA, FA, 1-ethyl-3-(3-(dimethylamino)propyl)-carbodiimide (EDC) hydrochloride, and sulfo-*N*-hydroxysuccinimide were purchased from Sigma-Aldrich (Madrid, Spain). Lipoid S75 (Phospholipids with 70% phosphatidylcholine) was purchased from Lipoid GmbH (Germany). Acetic acid (Scharlab, Barcelona, Spain), potassium hydroxide (Sigma-Aldrich, Madrid, Spain), potassium phosphate monobasic (Sigma-Aldrich, Madrid, Spain), and sodium phosphate dibasic (Sigma-Aldrich, Madrid, Spain) were used to prepare buffers of different pH. Vivaflow 50 Cassettes (Regenerated Cellulose, 100 kDa) and 0.2 μm filters (Regenerated Cellulose) were purchased from Sartorius Stedim Biotech (Göttingen, Germany). Acetonitrile HPLC Supragradient was purchased from Scharlab (Barcelona, Spain). Other chemicals were of analytical reagent grade and used without further purification.

5.2. Chemistry. Compound **1** was synthesized previously as a free base (23% yield, 98% purity) from 4-amino-*N*-(4-aminophenyl)benzamide and *S*-(2-naphthylmethyl)-2-pyridylthioimidate hydrobromide (Scheme 2).[5]

5.3. NLC Synthesis and Characterization. *5.3.1. Synthesis and Functionalization of NLC.* NLCs were synthesized by a modification of the warm microemulsion method previously described[60] using a microwave reactor (MW) (Biotage Initiator$^+$) (Scheme 1). Briefly, all components (Table S1) were weighed and placed in a microwave tube that was sealed. The reaction was then carried out in the MW reactor at 68 °C for 20 min, obtaining a clear microemulsion. The warm microemulsion was then dispersed in water at the same temperature (68 °C) at a ratio of 1:20 (v/v) under magnetic stirring (1250 rpm), and then it was left to cool down under magnetic stirring. A temperature <25 °C was achieved after 30 min. Obtained NLC dispersion was washed 3 times by TFF to eliminate nonincorporated drugs and excess excipients, using this technique also for volume reduction, reaching a final volume of NLC dispersion of 10 mL. In the case of NLC synthesized for later functionalization with FA, at this first step, the NLC dispersion was only concentrated by TFF until the reduction of initial volume to 10 mL.

The NLC surface was functionalized with FA by covalent linkage to the amine residues present on the NLC surface.[61,62] To do so, FA was added in a 2:1 molar ratio to ODA in HEPES 1 M (pH 7.5−8.0) in the presence of EDC and sulfo-*N*-hydroxysuccinimide (sulfo-NHS). The molar ratio between FA, EDC, and sulfo-NHS was 1:3:3.3. The reaction was left under magnetic stirring (700 rpm) for 4 h. At pre-established time points (0, 1, 2, 3, and 4 h), a sample was taken (0.5 mL) to evaluate the incorporation of FA. The sample was washed 3 times with an Amicon filtration system (100 kDa), and the HDD and zeta potential were measured. An effective addition of FA should cause an inversion of the NLC zeta potential from positive to negative.

At the end of the reaction, FA-functionalized NLCs were purified by washing 3 times by TFF as previously described to remove the excess reagents, obtaining a final volume of 10 mL.

The amount of FA attached to the NLC was determined spectrophotometrically at 280 nm by using a CLARIOstar Plus Microplate reader with a UV detector. To do so, FA-functionalized NLC was destroyed by dilution with methanol (1:20, v/v) to release attached FA. Then, the concentration of FA in FA-functionalized NLC was calculated with a calibration curve of FA in methanol (in the range of 1−42 μg/mL).

5.3.2. NLC Physicochemical Characterization. The HDD and PDI of all sets of NLC synthesized were assessed by photon correlation spectroscopy using a Zetasizer nano ZS90 instrument (Malvern Panalytical, UK). All measurements were performed in triplicate at RT. The surface charge or zeta potential of NLC was determined by Electrophoretic Light Scattering using a Zetasizer Nano ZS90 (Malvern Instruments, UK). For this, the NLCs were diluted in sodium chloride 100 mM (1:50) before the analyses. Each sample was analyzed in triplicate at RT.

The physical state of the lipid matrix was evaluated by DSC using a DSC 1 Star System Mettler-Toledo (Germany). An amount between 5−10 mg of raw lipid components, ODA, and glycerol monolaurate was weighted in an aluminum pan that was later sealed. A volume of NLC containing the equivalent

https://doi.org/10.1021/acsomega.4c08138
ACS Omega 2025, 10, 7795−7805

amount of these lipids was put in an aluminum pan, that was later sealed. DSC was carried out under N_2 flux using a temperature ramp of 5 °C/min from 30 to 90 °C.

5.3.3. Morphology Determination by TEM. The morphology of blank NLC and compound **1**-loaded NLC was examined by TEM. TEM analyses were performed at the National Centre of Electronic Microscopy of the Complutense University of Madrid (Madrid, Spain). NLCs were diluted 1:50 in water and placed on the surface of carbon-coated copper grids, negatively stained with 2% uranyl acetate, and observed under TEM using a JEOL JEM 1400 instrument operated at 100 kV equipped with a CCD camera Gatan Orius Sc 200.

5.3.4. Determination of Entrapment Efficiency. The concentration of compound **1**-loaded NLC, plain, and FA-functionalized NLC was determined before and after the purification process using TFF by means of HPLC−MS analysis using a SunFire C18 3.5 μm 2.1 × 50 mm column. The chromatography was carried out at a flow rate of 1 mL/min, using a gradient of water/acetonitrile (containing 0.02% formic acid) from 95/5 to 5/95 in t = 5 min. A calibration curve was obtained by dissolving **1** in ethyl acetate and diluting it in acetonitrile at different concentrations (0.5 μg/mL−15 μg/mL). The theoretical concentration of compound **1** loaded in the NLC is 150 μg/mL (10 mL of reaction volume). The analytical samples were prepared by dilution (1:50, v/v) of final NLC dispersion with acetonitrile (containing 0.02% formic acid) and then filtered with a 0.2 μm poly(ether sulfone) (PES) filter before analysis. This dilution step is required in the first instance to destroy the NLC and release the encapsulated compound **1** (analyte), using the selected dilution factor in order to fit the concentration of the analytical samples within the concentration range of the calibration curve. Entrapment efficiency (EE %) was calculated using the following formula

$$\mathbf{EE}\% = \frac{C_{AP}}{C_{BP}} \times 100$$

where C_{AP} is the concentration of **1** obtained after the purification process, and C_{BP} is the concentration of **1** before the purification process.

5.3.5. Drug Release In Vitro Evaluation. Compound **1** release from NLC at acidic and physiological pH was evaluated using low ionic strength buffers (pH 5.5 and 7.4) in order to ensure NLC stability during the study. NLCs were diluted 1:5 (v/v) in the corresponding buffer and incubated at 37 °C for 24 h. At pre-established time points, the released compound **1** was removed by centrifugation using an Amicon filtration system (membrane cutoff 100 kDa) and the remaining compound **1** was determined by NLC disruption and quantification by HPLC-MS, as described in Section 5.3.4. Moreover, the HDD at each time point was measured by DLS to check the integrity of the particles during the in vitro release study.

5.3.6. Stability Studies. All sets of prepared NLC formulations were subjected to stability studies in triplicate. NLC colloidal stability during storage was evaluated at RT by measurement of HDD, PDI, and zeta potential at pre-established time points over 60 days. Moreover, the behavior of **1**-loaded NLC in the culture medium selected for biological studies was also evaluated. To do so, NLCs were diluted 1:20, 1:50, 1:100, 1:500, and 1:1000 (v/v) and incubated at 37 °C for 24 h in not-supplemented DMEM, used for macrophages culture, and in SIM, used for *Leishmania* strain growth. At pre-established time points, the HDD and count rate were measured by DLS.

5.4. Biology. *5.4.1. Determination of Cellular Toxicity.* Cytotoxicity was carried out as previously described.[63−65] Briefly, counterscreening was performed against *Mus musculus* leukemia virus-transformed macrophage (RAW267.4) cells (ATCC TIB-71) cultured in DMEM (Fisher Scientific) supplemented with 10% HIFBS (Biosera). Cells were counted using a Neubauer Improved Hemocytometer. Plates were seeded with 5 × 10^3 cells per well. Following overnight incubation at 37 °C and 5% CO_2, cells were incubated with test compounds in 100 μL of media for 24 h in the same conditions and then for a further 4 h after adding 10 μL of alamarBlue. Subsequently, cell viability was assessed using a fluorescent plate reader (BioTek; 560EX nm/600 EM nm).

5.4.2. Assessing the Efficacy of Test Compounds against *L. mexicana*- or *L. major*-Infected Macrophages. *L. mexicana* (MNYC/BZ/62/M379) and *L. major* (MHOM/IL/81/Friedlin) were separately maintained at 26 °C in Schneider's Drosophila media (Sigma-Aldrich) supplemented with heat-inactivated fetal bovine serum (HIFBS; 15% for promastigotes, and 20% for amastigotes; Gibco). As previously described, *L. mexicana* promastigotes were transformed into axenic amastigotes by a pH and temperature shift.[64] On the other hand, metacyclic promastigotes of *L. major* were recovered during the stationary phase from the *L. major* promastigote cultures.

The efficacy of the NP, compound **1** alone, or control drug against *L. mexicana*- or *L. major*-infected macrophages was assessed as previously described[66] with modifications. Briefly, RAW264.7 (TIB-71, ATCC) cells were routinely cultured in $DMEM_{10}$ (10% FBS; 1% Penicillin−Streptomycin and 1% nonessential amino acids). Cells were later seeded in 96-well plates at 5 × 10^5 cells mL^{-1} (100 μL/well) density and incubated overnight at 37 °C, 5% CO_2, before being washed twice with 100 μL $DMEM_2$ (2% FBS, 1% PS). *L. mexicana* amastigotes or *L. major* metacyclic promastigotes at a concentration of 50 × 10^5 cells mL^{-1} (100 μL/well) resuspended in $DMEM_2$ were used to infect RAW264.7 cells, and plates were later incubated for another 24 h at 37 °C, 5% CO_2. Subsequently, infected *L. mexicana* or *L. major* cells were washed five times with $DMEM_2$ before being treated with serial dilutions of the test compounds in $DMEM_2$ in 100 μL final volume for a further 24 h incubation at 37 °C, 5% CO_2. Finally, the infected RAW264.7 cells were washed three times with serum-free SIM and lysed with 20 μL/well of SDS (0.05%, v/v in Schneider's media) for 30 s before addition of 180 μL/well of SIM (pH 7, 15% FBS). Plates were later Parafilm sealed and incubated for 48 h at 26 °C. Then, 10 μL of Resazurin (125 μg/mL) was added to each well before a 4 h incubation at 26 °C before assessing parasite viability using a fluorescent plate reader (BioTek; 560EX nm/600 EM nm). All of the experiments described above were carried out in triplicates.

5.4.3. Screening against Promastigotes and Amastigotes (or Metacyclic Promastigotes). Four ×10^4 parasites per well were seeded in a clear flat bottom 96-well microplate (Nunc Microwell; Fisher Scientific UK), excluding the outer wells. For the positive and negative controls, 0.5 μL of 1 mM Amphotericin B (Amp B; Sigma-Aldrich) or DMSO was added to each well. Serial dilutions of the NPs, compound **1** alone, or control drug were later introduced to a final volume of 100 μL

https://doi.org/10.1021/acsomega.4c08138
ACS Omega 2025, 10, 7795−7805

in each well and incubated at 26 °C for 24 h. Ten μL of Resazurin (125 μg/mL) was added to each well, followed by a further 24 h incubation. Plates were then read using the BioTek FLx800 fluorescence microplate reader (BioTek; 560EX nm/600 EM nm).

■ ASSOCIATED CONTENT

Data Availability Statement

The data that support the findings of this study are available throughout the manuscript and supporting files.

Supporting Information

The Supporting Information is available free of charge at https://pubs.acs.org/doi/10.1021/acsomega.4c08138.

Monitorization of FA functionalization process by changes in the NLC zeta potential (Figure S1), colloidal stability of 1-NLC formulation diluted in buffer at pH 5.5. and 7.4 (Figure S2), microemulsion composition for the synthesis of NLC (Table S1), and HPLC trace of compound **1** (PDF)

■ AUTHOR INFORMATION

Corresponding Authors

Christophe Dardonville − *Instituto de Química Médica, IQM−CSIC, E-28006 Madrid, Spain;* orcid.org/0000-0001-5395-1932; Phone: +34 912587490; Email: dardonville@iqm.csic.es

Ana González-Paredes − *Instituto de Química Médica, IQM−CSIC, E-28006 Madrid, Spain;* orcid.org/0000-0002-3504-0841; Phone: +34 912587552; Email: ana.gonzalez@iqm.csic.es

Authors

J. Jonathan Nué-Martinez − *Instituto de Química Médica, IQM−CSIC, E-28006 Madrid, Spain; PhD Programme in Medicinal Chemistry, Doctoral School, Universidad Complutense de Madrid, 28040 Madrid, Spain;* orcid.org/0000-0001-6483-6892

Marta Leo-Barriga − *Instituto de Química Médica, IQM−CSIC, E-28006 Madrid, Spain;* orcid.org/0000-0003-4853-5250

Fernando Herranz − *Instituto de Química Médica, IQM−CSIC, E-28006 Madrid, Spain; CIBER Enfermedades Respiratorias, 28029 Madrid, Spain;* orcid.org/0000-0002-3743-0050

Zisis Koutsogiannis − *Department of Biosciences, Durham University, Durham DH1 3LE, U.K.*

Paul W. Denny − *Department of Biosciences, Durham University, Durham DH1 3LE, U.K.;* orcid.org/0000-0002-5051-1613

Godwin U. Ebiloma − *School of Science, Engineering & Environment, University of Salford, Manchester M5 4WT, U.K.;* orcid.org/0000-0003-4072-9800

Complete contact information is available at: https://pubs.acs.org/10.1021/acsomega.4c08138

Author Contributions

Conception and design: JJN-M, FH, CD, and AG-P. Analysis and interpretation of the data: JJN-M, ML-B, ZK, PWD, GUE, CD, and AG-P. Drafting of the paper: JJN-M, ML-B, FH, ZK, PWD, GUE, CD, and AG-P. Final approval of the version to be published: JJN-M, ML-B, FH, ZK, PWD, GUE, CD, and AG-P. All authors agree to be accountable for all aspects of the work.

Funding

This study was supported by Agencia Estatal de Investigación (MCIN/AEI/10.13039/501100011033) and "ERDF A way of making Europe", by the "European Union", under grants RTI2018-093940-B-I00, PID2022-136438OB-I00, and PDC2022-133269-I00 (funded by the Recovery and Resilience Facility, RRF, NextGenerationEU) and Comunidad de Madrid (Spain) under "Atracción de Talento (Modalidad 1)" program (Reference 2019-T1/IND-12906).

Notes

The authors declare no competing financial interest.

Ethical approval statement: Axenic amastigotes were generated in vitro from reference strain *Leishmania mexicana* insect stage promastigotes using protocols and facilities to UK Health and Safety Executive standards. As such, no animals were involved in this study and ethical approval was not required.

■ ACKNOWLEDGMENTS

J.J.N.-M. was a recipient of a PhD fellowship from the Programa Nacional de Becas y Crédito Educativo (PRONABEC) of the Peruvian Government. G.U.E. and C.D. belong to the COST Action "OneHealthdrugs" CA21111.

■ ABBREVIATIONS USED

CL, cutaneous leishmaniasis; DMEM, Dulbecco's Modified Eagle's Medium; DSC, differential scanning calorimetry; FA, folic acid; FR, folate receptor; FR, folate transporter; HDD, hydrodynamic diameter; MGB, minor groove binder; kDNA, kinetoplast (mitochondrial) DNA; NP, nanoparticle; NCL, nanostructured carrier lipid; PDI, polydispersity index; SIM, Schneider's insect medium; SLN, solid lipid nanoparticle; TEM, transmission electron microscopy; TI, therapeutic index; VL, visceral leishmaniasis; ODA, octadecylamine; RT, room temperature; TFF, tangential flow filtration

■ REFERENCES

(1) Fact sheet: Leishmaniasis (World Health Organization). 2022. https://www.who.int/news-room/fact-sheets/detail/leishmaniasis (accessed 07 03, 2022).

(2) World Health Organization. *Working to overcome the global impact of neglected tropical diseases: first WHO report on neglected tropical diseases*; World Health Organization: Geneva, 2010. http://www.who.int/neglected_diseases/2010report/NTD_2010report_embargoed.pdf.

(3) Burza, S.; Croft, S. L.; Boelaert, M. Leishmaniasis. *Lancet* **2018**, *392* (10151), 951−970.

(4) Ponte-Sucre, A.; Gamarro, F.; Dujardin, J. C.; Barrett, M. P.; Lopez-Velez, R.; Garcia-Hernandez, R.; Pountain, A. W.; Mwenechanya, R.; Papadopoulou, B. Drug resistance and treatment failure in leishmaniasis: A 21st century challenge. *PLoS Neglected Trop. Dis.* **2017**, *11* (12), No. e0006052.

(5) Nué-Martinez, J. J.; Cisneros, D.; Moreno-Blázquez, M. d. V.; Fonseca-Berzal, C.; Manzano, J. I.; Kraeutler, D.; Ungogo, M. A.; Aloraini, M. A.; Elati, H. A. A.; Ibáñez-Escribano, A.; et al. Synthesis and biophysical and biological studies of N-phenylbenzamide derivatives targeting kinetoplastid parasites. *J. Med. Chem.* **2023**, *66* (19), 13452−13480.

(6) Millan, C. R.; Acosta-Reyes, F. J.; Lagartera, L.; Ebiloma, G.; Lemgruber, L.; Nué-Martinez, J. J.; Saperas, N.; Dardonville, C.; de Koning, H.; Campos, J. L. Functional and structural analysis of AT-specific minor groove binders that disrupt DNA-protein interactions

and cause disintegration of the *Trypanosoma brucei* kinetoplast. *Nucleic Acids Res.* **2017**, *45* (14), 8378−8391.
(7) Nué-Martinez, J. J.; Maturana, M.; Lagartera, L.; Rodríguez-Gutiérrez, J.-A.; Boer, R.; Campos, J. L.; Saperas, N.; Dardonville, C. Crystal structure of the HMGA AT-hook 1 domain bound to the minor groove of AT-rich DNA and inhibition by antikinetoplastid drugs. *Sci. Rep.* **2024**, *14* (1), 26173.
(8) Kelly, B. L.; Singh, G.; Aiyar, A. Molecular and cellular characterization of an AT-hook protein from *Leishmania*. *PLoS One* **2011**, *6* (6), No. e21412.
(9) Alvar, J.; Arana, B. Leishmaniasis, impact and therapeutic needs. In *Drug Discovery for Leishmaniasis*; Rivas, L., Gil, C., Eds.; The Royal Society of Chemistry, 2017.
(10) *Leishmaniasis en las Américas, Recomendaciones para el tratamiento*; PAHO; OPS/OMS, Organización Panamericana de la Salud: WA, 2013.
(11) McGwire, B. S.; Satoskar, A. R. Leishmaniasis: clinical syndromes and treatment. *Q. J. Med.* **2014**, *107* (1), 7−14.
(12) Castro, M. d. M.; Rode, J.; Machado, P. R. L.; Llanos-Cuentas, A.; Hueb, M.; Cota, G.; Rojas, I. V.; Orobio, Y.; Oviedo Sarmiento, O.; Rojas, E.; et al. Cutaneous leishmaniasis treatment and therapeutic outcomes in special populations: A collaborative retrospective study. *PLoS Neglected Trop. Dis.* **2023**, *17* (1), No. e0011029.
(13) Jamshaid, H.; Din, F. u.; Khan, G. M. Nanotechnology based solutions for anti-leishmanial impediments: a detailed insight. *J. Nanobiotechnol.* **2021**, *19* (1), 106.
(14) Salvi, V. R.; Pawar, P. Nanostructured lipid carriers (NLC) system: A novel drug targeting carrier. *J. Drug Delivery Sci. Technol.* **2019**, *51*, 255−267.
(15) Patel, P.; Patel, M. Nanostructured Lipid Carriers- A versatile carrier for oral delivery of lipophilic drugs. *Recent Pat. Nanotechnol.* **2021**, *15* (2), 154−164.
(16) de Souza, A.; Yukuyama, M. N.; Barbosa, E. J.; Monteiro, L. M.; Faloppa, A. C. B.; Calixto, L. A.; de Barros Araujo, G. L.; Fotaki, N.; Lobenberg, R.; Bou-Chacra, N. A. A new medium-throughput screening design approach for the development of hydroxymethylnitrofurazone (NFOH) nanostructured lipid carrier for treating leishmaniasis. *Colloids Surf., B* **2020**, *193*, 111097.
(17) Galvão, J. G.; Santos, R. L.; Silva, A.; Santos, J. S.; Costa, A. M. B.; Chandasana, H.; Andrade-Neto, V. V.; Torres-Santos, E. C.; Lira, A. A. M.; Dolabella, S.; et al. Carvacrol loaded nanostructured lipid carriers as a promising parenteral formulation for leishmaniasis treatment. *Eur. J. Pharm. Sci.* **2020**, *150*, 105335.
(18) Jesus, J. A.; Sousa, I. M. O.; da Silva, T. N. F.; Ferreira, A. F.; Laurenti, M. D.; Antonangelo, L.; Faria, C. S.; da Costa, P. C.; de Carvalho Ferreira, D.; Passero, L. F. D. Preclinical assessment of ursolic acid loaded into nanostructured lipid carriers in experimental visceral leishmaniasis. *Pharmaceutics* **2021**, *13* (6), 908.
(19) Das, S.; Ghosh, S.; De, A. K.; Bera, T. Oral delivery of ursolic acid-loaded nanostructured lipid carrier coated with chitosan oligosaccharides: Development, characterization, in vitro and in vivo assessment for the therapy of leishmaniasis. *Int. J. Biol. Macromol.* **2017**, *102*, 996−1008.
(20) Etxebeste-Mitxeltorena, M.; Moreno, E.; Carvalheiro, M.; Calvo, A.; Navarro-Blasco, I.; González-Peñas, E.; Álvarez-Galindo, J. I.; Plano, D.; Irache, J. M.; Almeida, A. J.; et al. Oral efficacy of a diselenide compound loaded in nanostructured lipid carriers in a murine model of visceral leishmaniasis. *ACS Infect. Dis.* **2021**, *7* (12), 3197−3209.
(21) Khan, A. S.; Ud Din, F.; Ali, Z.; Bibi, M.; Zahid, F.; Zeb, A.; Mujeeb, U. R.; Khan, G. M. Development, in vitro and in vivo evaluation of miltefosine loaded nanostructured lipid carriers for the treatment of cutaneous leishmaniasis. *Int. J. Pharm.* **2021**, *593*, 120109.
(22) Riaz, A.; Hendricks, S.; Elbrink, K.; Guy, C.; Maes, L.; Ahmed, N.; Kiekens, F.; Khan, G. M. Preparation and characterization of nanostructured lipid carriers for improved topical drug delivery: evaluation in cutaneous leishmaniasis and vaginal candidiasis animal models. *AAPS PharmSciTech* **2020**, *21* (5), 185.
(23) Ferreira, M. A.; de Almeida Junior, R. F.; Onofre, T. S.; Casadei, B. R.; Farias, K. J. S.; Severino, P.; de Oliveira Franco, C. F.; Raffin, F. N.; de Lima e Moura, T. F. A.; de Melo Barbosa, R. Annatto oil loaded nanostructured lipid carriers: a potential new treatment for cutaneous leishmaniasis. *Pharmaceutics* **2021**, *13* (11), 1912.
(24) Unciti-Broceta, J. D.; Arias, J. L.; Maceira, J.; Soriano, M.; Ortiz-González, M.; Hernández-Quero, J.; Muñóz-Torres, M.; de Koning, H. P.; Magez, S.; Garcia-Salcedo, J. A. Specific cell targeting therapy bypasses drug resistance mechanisms in African trypanosomiasis. *PLoS Pathog.* **2015**, *11* (6), No. e1004942.
(25) Lüscher, A.; de Koning, H. P.; Mäser, P. Chemotherapeutic strategies against *Trypanosoma brucei*: drug targets vs. drug targeting. *Curr. Pharm. Des.* **2007**, *13* (6), 555−567.
(26) Chowdhary, S. J.; Chowdhary, A.; Kashaw, S. Macrophage targeting: a strategy for leishmaniasis specific delivery. *Int. J. Pharm. Pharm. Sci.* **2016**, *8* (2), 16−26.
(27) Barrett, M. P.; Gilbert, I. H. Targeting of toxic compounds to the trypanosome's interior. *Adv. Parasitol.* **2006**, *63*, 125−183.
(28) Vickers, T. J.; Beverley, S. M. Folate metabolic pathways in *Leishmania*. *Essays Biochem.* **2011**, *51*, 63−80.
(29) Cunningham, M. L.; Beverley, S. M. Pteridine salvage throughout the *Leishmania* infectious cycle: implications for antifolate chemotherapy. *Mol. Biochem. Parasitol.* **2001**, *113* (2), 199−213.
(30) Elnakat, H.; Ratnam, M. Distribution, functionality and gene regulation of folate receptor isoforms: implications in targeted therapy. *Adv. Drug Delivery Rev.* **2004**, *56* (8), 1067−1084.
(31) Jain, N. K.; Mishra, V.; Mehra, N. K. Targeted drug delivery to macrophages. *Expert Opin. Drug Delivery* **2013**, *10* (3), 353−367.
(32) Varghese, B.; Vlashi, E.; Xia, W.; Ayala Lopez, W.; Paulos, C. M.; Reddy, J.; Xu, L.-C.; Low, P. S. Folate receptor-β in activated macrophages: ligand binding and receptor recycling kinetics. *Mol. Pharmaceutics* **2014**, *11* (10), 3609−3616.
(33) Carron, P. M.; Crowley, A.; O'Shea, D.; McCann, M.; Howe, O.; Hunt, M.; Devereux, M. Targeting the folate receptor: improving efficacy in inorganic medicinal chemistry. *Curr. Med. Chem.* **2018**, *25* (23), 2675−2708.
(34) Cohen-Freue, G.; Holzer, T. R.; Forney, J. D.; McMaster, W. R. Global gene expression in *Leishmania*. *Int. J. Parasitol.* **2007**, *37* (10), 1077−1086.
(35) Mallinson, D. J.; Coombs, G. H. Biochemical characteristics of the metacyclic forms of *Leishmania major* and *L. mexicana mexicana*. *Parasitology* **1989**, *98* (1), 7−15.
(36) Madusanka, R. K.; Silva, H.; Karunaweera, N. D. Treatment of cutaneous leishmaniasis and insights into species-specific responses: a narrative review. *Infect. Dis. Ther.* **2022**, *11* (2), 695−711.
(37) Navin, T. R.; Arana, B. A.; Arana, F. E.; Berman, J. D.; Chajón, J. F. Placebo-controlled clinical trial of sodium stibogluconate (pentostam) versus ketoconazole for treating cutaneous leishmaniasis in Guatemala. *J. Infect. Dis.* **1992**, *165* (3), 528−534.
(38) Galvão, E. L.; Rabello, A.; Cota, G. F. Efficacy of azole therapy for tegumentary leishmaniasis: A systematic review and meta-analysis. *PLoS One* **2017**, *12* (10), No. e0186117.
(39) Escobar, P.; Matu, S.; Marques, C.; Croft, S. L. Sensitivities of *Leishmania* species to hexadecylphosphocholine (miltefosine), ET-18-OCH3 (edelfosine) and amphotericin B. *Acta Trop.* **2002**, *81* (2), 151−157.
(40) Smith, L.; Serrano, D. R.; Mauger, M.; Bolás-Fernández, F.; Dea-Ayuela, M. A.; Lalatsa, A. Orally bioavailable and effective buparvaquone lipid-based nanomedicines for visceral leishmaniasis. *Mol. Pharmaceutics* **2018**, *15* (7), 2570−2583.
(41) Monteiro, L. M.; Löbenberg, R.; Cotrim, P. C.; Barros de Araujo, G. L.; Bou-Chacra, N. Buparvaquone nanostructured lipid carrier: development of an affordable delivery system for the treatment of leishmaniases. *BioMed. Res. Int.* **2017**, *2017*, 9781603.
(42) Kar, N.; Chakraborty, S.; De, A. K.; Ghosh, S.; Bera, T. Development and evaluation of a cedrol-loaded nanostructured lipid carrier system for *in vitro* and *in vivo* susceptibilities of wild and drug resistant *Leishmania donovani* amastigotes. *Eur. J. Pharm. Sci.* **2017**, *104*, 196−211.

https://doi.org/10.1021/acsomega.4c08138
ACS Omega 2025, 10, 7795−7805

(43) Hirsjärvi, S.; Sancey, L.; Dufort, S.; Belloche, C.; Vanpouille-Box, C.; Garcion, E.; Coll, J. L.; Hindré, F.; Benoît, J. P. Effect of particle size on the biodistribution of lipid nanocapsules: comparison between nuclear and fluorescence imaging and counting. *Int. J. Pharm.* **2013**, *453* (2), 594−600.
(44) Troncoso, E.; Aguilera, J. M.; McClements, D. J. Influence of particle size on the *in vitro* digestibility of protein-coated lipid nanoparticles. *J. Colloid Interface Sci.* **2012**, *382* (1), 110−116.
(45) Cabral, H.; Matsumoto, Y.; Mizuno, K.; Chen, Q.; Murakami, M.; Kimura, M.; Terada, Y.; Kano, M. R.; Miyazono, K.; Uesaka, M.; et al. Accumulation of sub-100 nm polymeric micelles in poorly permeable tumours depends on size. *Nat. Nanotechnol.* **2011**, *6* (12), 815−823.
(46) Yardley, V.; Croft, S. L. Activity of liposomal amphotericin B against experimental cutaneous leishmaniasis. *Antimicrob. Agents Chemother.* **1997**, *41* (4), 752−756.
(47) Rebouças-Silva, J.; Tadini, M. C.; Devequi-Nunes, D.; Mansur, A. L.; S Silveira-Mattos, P.; I de Oliveira, C.; R Formiga, F.; Berretta, A. A.; Marquele-Oliveira, F.; Borges, V. M. Evaluation of in vitro and in vivo efficacy of a novel amphotericin B-loaded nanostructured lipid carrier in the treatment of *Leishmania braziliensis* infection. *Int. J. Nanomed.* **2020**, *15*, 8659−8672.
(48) Richard, D.; Leprohon, P.; Drummelsmith, J.; Ouellette, M. Growth phase regulation of the main folate transporter of *Leishmania infantum* and its role in methotrexate resistance. *J. Biol. Chem.* **2004**, *279* (52), 54494−54501.
(49) Richard, D.; Kündig, C.; Ouellette, M. A new type of high affinity folic acid transporter in the protozoan parasite *Leishmania* and deletion of its gene in methotrexate-resistant cells. *J. Biol. Chem.* **2002**, *277* (33), 29460−29467.
(50) Pauraic, M. C.; Aisling, C.; Denis, O. S.; Malachy, M.; Orla, H.; Mary, H.; Michael, D. Targeting the folate receptor: improving efficacy in inorganic medicinal chemistry. *Curr. Med. Chem.* **2018**, *25*, 2675.
(51) Bahrami, B.; Mohammadnia-Afrouzi, M.; Bakhshaei, P.; Yazdani, Y.; Ghalamfarsa, G.; Yousefi, M.; Sadreddini, S.; Jadidi-Niaragh, F.; Hojjat-Farsangi, M. Folate-conjugated nanoparticles as a potent therapeutic approach in targeted cancer therapy. *Tumor Biol.* **2015**, *36* (8), 5727−5742.
(52) Zwicke, G. L.; Ali Mansoori, G.; Jeffery, C. J. Utilizing the folate receptor for active targeting of cancer nanotherapeutics. *Nano Rev.* **2012**, *3*, 18496.
(53) Jain, V.; Gupta, A.; Pawar, V. K.; Asthana, S.; Jaiswal, A. K.; Dube, A.; Chourasia, M. K. Chitosan-assisted immunotherapy for intervention of experimental leishmaniasis via amphotericin B-loaded solid lipid nanoparticles. *Appl. Biochem. Biotechnol.* **2014**, *174* (4), 1309−1330.
(54) Pires, V. C.; Magalhães, C. P.; Ferrante, M.; Rebouças, J. d. S.; Nguewa, P.; Severino, P.; Barral, A.; Veras, P. S. T.; Formiga, F. R. Solid lipid nanoparticles as a novel formulation approach for tanespimycin (17-AAG) against *Leishmania* infections: Preparation, characterization and macrophage uptake. *Acta Trop.* **2020**, *211*, 105595.
(55) Fröhlich, E. The role of surface charge in cellular uptake and cytotoxicity of medical nanoparticles. *Int. J. Nanomed.* **2012**, *7*, 5577−5591.
(56) Oliveira, D. M.; Furtado, F. B.; Gomes, A. A. S.; Belut, B. R.; Nascimento, E. A.; Morais, S. A. L.; Martins, C. H. G.; Santos, V. C. O.; da Silva, C. V.; Teixeira, T. L.; et al. Chemical constituents and antileishmanial and antibacterial activities of essential oils from *Scheelea phalerata*. *ACS Omega* **2020**, *5* (3), 1363−1370.
(57) Serrano, D. R.; Lalatsa, A.; Dea-Ayuela, M. A. Engineering synergistically active and bioavailable cost-effective medicines for neglected tropical diseases; the role of excipients. *Curr. Top. Med. Chem.* **2017**, *17*, 2888.
(58) Araujo, V. H. S.; da Silva, P. B.; Szlachetka, I. O.; da Silva, S. W.; Fonseca-Santos, B.; Chorilli, M.; Ganassin, R.; de Oliveira, G. R. T.; da Rocha, M. C. O.; Fernandes, R. P.; et al. The influence of NLC composition on curcumin loading under a physicochemical perspective and in vitro evaluation. *Colloids Surf., A* **2020**, *602*, 125070.
(59) Song, A.; Zhang, X.; Li, Y.; Mao, X.; Han, F. Effect of liquid-to-solid lipid ratio on characterizations of flurbiprofen-loaded solid lipid nanoparticles (SLNs) and nanostructured lipid carriers (NLCs) for transdermal administration. *Drug Dev. Ind. Pharm.* **2016**, *42* (8), 1308−1314.
(60) Chinigò, G.; Gonzalez-Paredes, A.; Gilardino, A.; Barbero, N.; Barolo, C.; Gasco, P.; Fiorio Pla, A.; Visentin, S. Polymethine dyes-loaded solid lipid nanoparticles (SLN) as promising photosensitizers for biomedical applications. *Spectrochim. Acta, Part A* **2022**, *271*, 120909.
(61) Lomant, A. J.; Fairbanks, G. Chemical probes of extended biological structures: Synthesis and properties of the cleavable protein cross-linking reagent [35S]dithiobis(succinimidyl propionate). *J. Mol. Biol.* **1976**, *104* (1), 243−261.
(62) Staros, J. V.; Wright, R. W.; Swingle, D. M. Enhancement by *N*-hydroxysulfosuccinimide of water-soluble carbodiimide-mediated coupling reactions. *Anal. Biochem.* **1986**, *156* (1), 220−222.
(63) Anderson, O.; Beckett, J.; Briggs, C. C.; Natrass, L. A.; Cranston, C. F.; Wilkinson, E. J.; Owen, J. H.; Mir Williams, R.; Loukaidis, A.; Bouillon, M. E.; et al. An investigation of the antileishmanial properties of semi-synthetic saponins. *RSC Med. Chem.* **2020**, *11* (7), 833−842.
(64) Treiger Borborema, S. E.; Schwendener, R. A.; Osso Junior, J. A.; de Andrade Junior, H. F.; do Nascimento, N. Uptake and antileishmanial activity of meglumine antimoniate-containing liposomes in *Leishmania (Leishmania) major*-infected macrophages. *Int. J. Antimicrob. Agents* **2011**, *38* (4), 341−347.
(65) Zheng, Z. W.; Li, J.; Chen, H.; He, J. L.; Chen, Q. W.; Zhang, J. H.; Zhou, Q.; Chen, D. L.; Chen, J. P. Evaluation of in vitro antileishmanial efficacy of cyclosporin A and its non-immunosuppressive derivative, dihydrocyclosporin A. *Parasites Vectors* **2020**, *13* (1), 94.
(66) Eggimann, G. A.; Bolt, H. L.; Denny, P. W.; Cobb, S. L. Investigating the anti-leishmanial effects of linear peptoids. *ChemMedChem* **2015**, *10* (2), 233−237.

https://doi.org/10.1021/acsomega.4c08138
ACS Omega 2025, 10, 7795−7805